

Deep Clustering with Diffused Sampling and Hardness-aware Self-distillation

Hai-Xin Zhang, Dong Huang, *Member, IEEE*

Abstract—Deep clustering has gained significant attention due to its capability in learning clustering-friendly representations without labeled data. However, previous deep clustering methods tend to treat all samples equally, which neglect the variance in the latent distribution and the varying difficulty in classifying or clustering different samples. To address this, this paper proposes a novel end-to-end deep clustering method with diffused sampling and hardness-aware self-distillation (HaDis). Specifically, we first align one view of instances with another view via diffused sampling alignment (DSA), which helps improve the intra-cluster compactness. To alleviate the sampling bias, we present the hardness-aware self-distillation (HSD) mechanism to mine the hardest positive and negative samples and adaptively adjust their weights in a self-distillation fashion, which is able to deal with the potential imbalance in sample contributions during optimization. Further, the prototypical contrastive learning is incorporated to simultaneously enhance the inter-cluster separability and intra-cluster compactness. Experimental results on five challenging image datasets demonstrate the superior clustering performance of our HaDis method over the state-of-the-art. Source code is available at <https://github.com/Regan-Zhang/HaDis>.

Index Terms—Deep clustering, Image clustering, Self-supervised learning, Contrastive learning, Hard sample mining, Self-distillation.

I. INTRODUCTION

Due to its remarkable ability to learn discriminative representations without ground-truth labels, deep clustering has gained significant attention in the field of representation learning and clustering. The rapid progress of deep clustering greatly benefits from the representation learning capabilities of self-supervised learning, which encompasses both contrastive learning [1], [2] and non-contrastive learning [3]–[5].

In recent years, the contrastive learning has become a predominant technique in many deep clustering methods [6]–[10]. Specifically, these existing deep clustering methods are often built upon some classical contrastive learning models like SimCLR [1], which requires a symmetric (weight-sharing) network architecture and a well-designed loss function. However, these contrastive learning based deep clustering methods necessitate the construction of a substantial number of negative pairs to learn representations to distinguish all instances in the embedding space.

Unlike the contrastive architecture, the non-contrastive deep clustering methods [3], [4] do not require any negative pairs but use the representation of one augmented view to align the other, which have also achieve considerable progress recently

[11]–[13]. Specifically, they typically adopt an asymmetric network architecture to perform representation learning and discriminative clustering simultaneously. Different from the symmetric networks, the asymmetric architecture usually contains a common network and a momentum network with stop-gradient.

Despite the promising ability of these previous contrastive and non-contrastive deep clustering methods, a common limitation to them is that they generally treat each data sample equally, lacking an adaptive evaluation of the clustering difficulty for individual samples. They tend to directly categorize samples into positive or negative pairs and simply assign them equal weights, disregarding the fact that different samples contribute differently to the model optimization, which is called the *sampling bias phenomenon* [14], [15]. How to balance the relationship between the contrastive learning and non-contrastive learning paradigms and alleviate the sampling bias phenomenon is still a challenging problem in deep clustering.

To address this, we propose a novel end-to-end deep clustering framework with diffused sampling and hardness-aware self-distillation, termed **HaDis**. Specifically, we propose diffused sampling alignment (DSA) to align one sample with its neighboring sample, which takes advantage of non-contrastive learning, successfully eliminating the reliance on a large number of negative samples and leading to improved compactness of the intra-cluster. Considering the hard samples play a crucial role in optimization [16], we propose hardness-aware self-distillation (HSD) to mitigate the sampling bias phenomenon elaborately, which first mines the hardest positive and negative samples simultaneously and then corrects the bias for them adaptively in a self-distillation fashion. Unlike some clustering algorithms [6], [9] and knowledge distillation methods [17], [18] requiring an additional pre-training stage or a well-trained teacher model, our HaDis is pretraining-free, as its teacher network gradually updates along with the student network. Furthermore, to avoid collapse and unstable clustering [12], we introduce prototypical contrastive learning (PCL) [11], [12] into our framework, which conducts contrastive learning at the prototype-level, leading to enhancing both the efficiency of clustering and the quality of clustering results.

The main contributions of our work are summarized as follows:

- We propose a novel end-to-end deep clustering framework, termed HaDis, which enjoys the benefits of both contrastive and non-contrastive learning and remedies their deficiencies: exclusion of massive negative pairs, well-concentrated intra-cluster, well-separated clusters and robust clustering stability.

H.-X. Zhang, D. Huang are with the College of Mathematics and Informatics, South China Agricultural University, Guangzhou, China.
E-mail: reganzhx@gmail.com, huangdonghere@gmail.com.

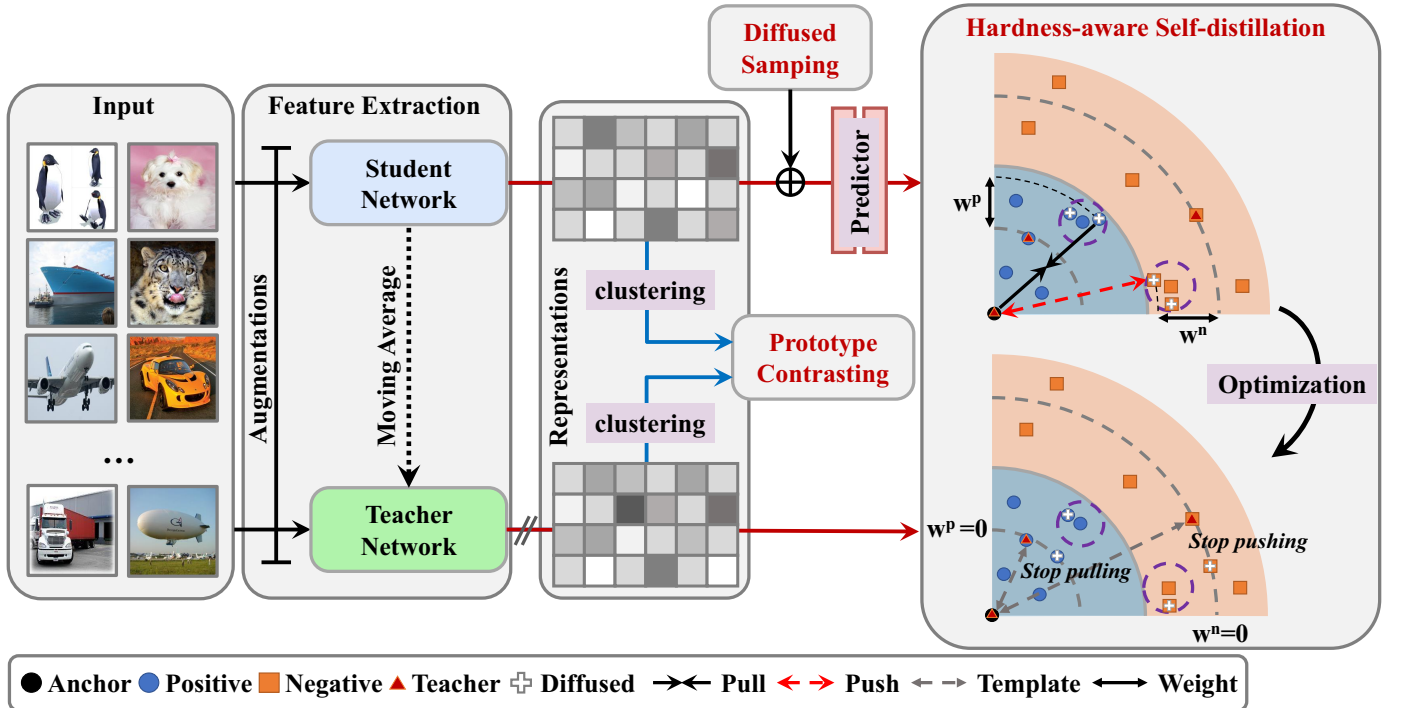


Fig. 1. The overall framework of our proposed HaDis framework.

- We propose diffused sampling alignment (DSA) to enhance instance alignment by considering neighboring positive samples in the embedding space, aiming to improve the intra-cluster compactness.
- We propose hardness-aware self-distillation (HSD) to mitigate the sampling bias phenomenon in a pretraining-free manner, which mines the hardest positive and negative samples simultaneously and corrects the weights for them adaptively.
- By incorporating prototypical contrastive learning (PCL), our HaDis outperforms the existing state-of-the-art methods. Extensive experiments on five challenging benchmark datasets demonstrate the superiority and efficiency of our proposed approach.

II. RELATED WORK

In this section, we conducted a brief survey on deep clustering, contrastive learning and hard sample learning.

A. Deep Clustering

Clustering is one of the fundamental tasks in unsupervised learning, which aims to partition the samples into clusters based on their similarities. The traditional clustering methods such as K -means, spectral clustering (SC) [19], agglomerative clustering (AC) [20] and nonnegative matrix factorization (NMF) [21] are typically designed for low-dimensional data, lacking of ability to handle high-dimensional complex data (e.g., image data).

Thanks to the strong representability of deep neural networks (DNN), deep clustering methods have indeed demonstrated notable advantages over traditional clustering algorithms, particularly in the realm of computer vision. Early

deep clustering methods only utilized a shallow network [22], [23] and a specialized clustering loss for learning clustering-friendly representations. For example, DEC [24] first utilizes the reconstruction loss to pre-train an auto-encoder network and then refines the cluster assignments with a KL-divergence based clustering loss. Further, [25] introduced joint unsupervised learning (JULE), which adopts a recurrent framework to learn discriminative representations and image clusters jointly. To solve the problem that unavoidable errors present in the neighborhoods, [26] proposed PICA to maximize the global partition confidence of clustering solution.

Recently, deep clustering has made significant progress with the assistance of contrastive learning. Some deep clustering methods based on contrastive learning have achieved remarkable performance [7], [8], [10], [12], [13]. Specifically, [8] presented the IDFD method to learn similarities among instances and reduce correlations within features by adopting the idea of instance discrimination [27] and spectral clustering [19].

To the best of our knowledge, CC [7] is the first work to conduct contrastive learning at both the instance- and cluster-level simultaneously. Subsequently, several excellent deep clustering works have emerged building upon the foundation of CC. Especially, [13] expanded the dual-branch structure of CC to a triple-branch structure and proposed a tri-stream clustering network called HTCEN. Besides, the work presented in the SACC [10] explored the impact of strong and weak augmentations on contrastive clustering. [12] proposed a clustering framework with prototype scattering loss and positive sampling alignment, termed ProPos, which enjoys the strengths of contrastive and non-contrastive learning.

B. Contrastive Learning

Recently, contrastive learning has emerged as a popular approach in representation learning, enabling the training of deep neural networks without relying on labeled data. The key idea of contrastive learning is to maximize the similarity between the representations of positive pairs while minimizing the similarity between that of negative pairs.

One of the pioneering works in contrastive learning is SimCLR [1], which introduced a simple framework for self-supervised learning using NT-Xent loss [28]. Building upon the success of SimCLR, subsequent works [2]–[5] have further improved contrastive learning techniques. Specifically, MoCo [2] utilizes an extra dynamic queue to store representations of negative samples and transforms contrastive learning into a key-value matching problem. Besides, MoCo employs a momentum update mechanism to stabilize the learning process, which has been proven effective in enhancing the quality of learned representations.

Compared to previous contrastive learning methods that require a large number of negative pairs, BYOL [3] stands out by eliminating the need for explicit negative pairs. Instead, BYOL solely aligns the representations obtained by its two networks. Further, SwAV [5] adopts a clustering-based objective to iteratively swap assignments between multiple views of each instance to refine the alignment. [4] summarized the aforementioned contrastive learning methods and proposed SimSiam to simplify contrastive learning methods and improve their performance. Similar to BYOL, SimSiam [4] only forces one view from the online network to predict another view from the target network, but removes the momentum updating mechanism.

C. Hard Sample Mining

In the field of contrastive learning, it has been proven that hard samples play a crucial role in achieving promising performance [16]. Previous studies [14], [29], [30] on image data have demonstrated the significance of hard negative samples, which is hard for optimization but useful for improving the robustness of the model.

On the other hand, this success has motivated researchers to explore the concept of hard negative sample mining on graph data. Concretely, [15] proposed GDCL to modify the bias for negative samples by applying the clustering pseudo-labels, aiming to decrease the false-negative samples. Recently, [31] proposed a graph contrastive learning method ProGCL, which employs a specialized measure to assess the hardness of negative samples, incorporating similarity information through a carefully designed probability estimator. More recently, [32] illuminated that overlooking hard positive samples would lead to sub-optimal performance in contrastive learning and proposed HSAN to focus on both hard positive and negative pairs.

Although the aforementioned methods have demonstrated their effectiveness, they often rely on pseudo-labels obtained by clustering to mine positive and negative samples, which increases the training burden and decreases the efficiency of learning from hard samples. To address this problem,

an efficient and self-adaptive metric strategy is proposed in hardness-aware self-distillation, which identifies the positive and negative samples via Euclidean distance between the embeddings of samples instead of clustering pseudo-labels, and adaptively calibrates the weights of hard samples to help model harness different difficulty of individual samples for clustering.

III. PROPOSED FRAMEWORK

A. Diffused Sampling Alignment

Contrary to contrastive learning, which relies heavily on the construction of a large number of negative samples, non-contrastive learning only necessitates positive samples and forces the representations of one view to align another [3], [4]. Moreover, it has been demonstrated that negative samples are not essential for representation learning [3], [4], [33]. Specifically, non-contrastive frameworks commonly utilize an online, a target, and a predictor network to establish a connection between these two views. And they employ a stop-gradient operation to prevent representation collapse.

In this paper, we propose diffused sampling alignment (DSA) to improve the intra-cluster compactness, which enjoys the strength of non-contrastive learning [3], [4], [33]. Further, we will utilize a self-distillation perspective to critically analyze non-contrastive learning. Specifically, the online network can be referred to as the student network and the target network as the teacher network. Formally, let $g(\cdot)$, $f_s(\cdot)$ and $f_t(\cdot)$ denote the predictor, the student network, and the teacher network respectively. Then assume that we have one instance x and its augmented view x^+ randomly generated from data augmentation. Hence, if the temperature coefficient $\tau = 0.5$, the loss used in BYOL [3] and SimSiam [4] can be reformulated as:

$$-2g(f_s(x))^T f_t(x^+) = \|g(f_s(x)) - f_t(x^+)\|_2^2 - 2, \quad (1)$$

where $g(f_s(x))$ and $f_t(x^+)$ are ℓ_2 -normalized.

Based on the assumption that neighboring samples around one view are *truly positive* with respect to its augmented view [12], we propose diffused sampling to spread the current features to the domain to generate diffused features. The key goal of DSA is to generate the diffused features. Specifically, following [12], we achieve the generation of diffused features by introducing a Gaussian distribution, which can be expressed as follows,

$$z = f_s(x) + \epsilon\delta, \quad \delta \sim \mathcal{N}(0, I), \quad (2)$$

where I denotes the identity matrix and ϵ is a hyperparameter controlling the extent of diffusion. Thus the loss in Eq. (1) is extended by applying the diffused features, which can be reformulated as:

$$\begin{aligned} \mathcal{L}_{DSA} &= \|g(z) - f_t(x^+)\|_2^2 \\ &= \|g(f_s(x) + \epsilon\delta) - f_t(x^+)\|_2^2, \end{aligned} \quad (3)$$

Note that when $\epsilon = 0$, \mathcal{L}_{DSA} reduces to Eq. (1).

B. Hardness-aware Self-distillation

Although it is known that the hard samples play a significant role in optimization [16], [17], the main challenge lies in how to excavate hard samples from the unlabeled data. Moreover, unlike the algorithms in knowledge distillation having a well-trained teacher model [17], [18], the teacher model in self-distillation is randomly initialized and trained from scratch. This results in the student network is required to learn discriminative knowledge without the supervision of the teacher network, which undoubtedly intensifies the difficulty of this challenge. To tackle this challenge, we propose hardness-aware self-distillation (HSD) to mine both hardest positive and negative samples simultaneously and try to fill the gap between the teacher and student networks with self-distillation.

Inspired by SMD [17], we adopt a teacher-guided metric strategy to mine positive and negative samples in an unsupervised manner. Formally, given the anchor x_i and another image x_a , we calculate their embeddings in the teacher network, namely, $f_t(x_i)$ and $f_t(x_a)$. We utilize a metric function $\mathcal{D}(\cdot)$ to measure the distance between two images in the embedding space. Following [17], we also apply the Euclidean distance to evaluate the similarity between two embeddings $\mathcal{D}(f_t(x_i), f_t(x_j)) = \|\bar{f}(x_i) - \bar{f}(x_j)\|_2$, in which $\bar{f}(x_i)$ and $\bar{f}(x_j)$ are normalized and a larger \mathcal{D} indicates a lower similarity between two features.

Theoretically, $\mathcal{D}(f_t(x_i), f_t(x_a))$ should be small if x_i and x_a belong to the same cluster. When $\mathcal{D}(f_t(x_i), f_t(x_a))$ is smaller (larger) than a decision boundary [34], x_i and x_a will be identified as a positive (negative) pair. Hence, the decision boundary about \mathcal{D} is essential. However, it is impossible to distinguish all positive and negative pairs with only a certain decision boundary or a hyperparameter. Further, in our self-distillation framework, the teacher network $f_t(\cdot)$ and the student network $f_s(\cdot)$ are randomly initialized and trained from scratch, which makes it so difficult to match $f_t(x_i)$ and $f_s(x_i)$ perfectly.

To solve this problem, we adopt a teacher-guided metric strategy to fill the gap between the teacher and student network, which is defined as follows:

$$(x_i, x_a) \in \begin{cases} \mathcal{G}_i^p, & \mathcal{D}(f_t(x_i), f_t(x_a)) < \mathcal{D}(f_t(x_i), g(z_a)), \\ \mathcal{G}_i^n, & \mathcal{D}(f_t(x_i), f_t(x_a)) \geq \mathcal{D}(f_t(x_i), g(z_a)), \end{cases} \quad (4)$$

where $g(\cdot)$ is the predictor, we denote $z_a = f_s(x_a) + \epsilon\delta$ for brevity, \mathcal{G}_i^p and \mathcal{G}_i^n are the positive set and the negative set, respectively.

The major purpose of our self-distillation is to pull the positive pair x_i and x_j closer while pushing negative pair x_i and x_m far away, where $j \in J$ and $m \in M$. Here, J and M represent the number of samples in \mathcal{G}_i^p and \mathcal{G}_i^n , respectively. To simplify matters, we employ the shorthand notation: $\nu_{ij}^p = \mathcal{D}(f_t(x_i), g(z_j))$, $\nu_{im}^n = \mathcal{D}(f_t(x_i), g(z_m))$. Thus the learning target is to minimize all ν_{ij}^p values while maximizing all ν_{im}^n .

Considering optimizing for all sample pairs, even within a batch, is computationally expensive and cost-prohibitive, we retain the most challenging positive and negative samples

while discarding the influence of other samples [16], [17]. Logically, the online mining process for the hardest samples is formulated as:

$$\nu_i^p = \max_{j \in \mathcal{G}_i^p} \nu_{ij}^p, \quad \nu_i^n = \min_{m \in \mathcal{G}_i^n} \nu_{im}^n, \quad (5)$$

where ν_i^p and ν_i^n stand for the hardest positive and negative pair excavated from the embedding space of the student network for anchor x_i .

In practice, it is inevitable that there will be erroneous samples present. The accumulation of these erroneous samples can significantly impact the performance of the model, potentially leading to sub-optimal results or even model collapse. To solve this problem, we adopt a teacher-guided self-adaptive weighting mechanism [17]. This mechanism adaptively re-allocates the contribution of different ν_i^p and ν_i^n during the training process.

Formally, for an anchor x_i , we obtain its corresponding hardest positive x_{j^h} and hardest negative x_{m^h} from \mathcal{G}_i^p and \mathcal{G}_i^n . Thus we define the rule of teacher-guided self-adaptive weighting mechanism as:

$$\begin{cases} w_i^p = \max(\nu_i^p - \mathcal{D}(f_t(x_i), f_t(x_{j^h})), 0), \\ w_i^n = \max(\mathcal{D}(f_t(x_i), f_t(x_{m^h})) - \nu_i^n, 0), \end{cases} \quad (6)$$

where $\mathcal{D}(f_t(x_i), f_t(x_{j^h}))$ and $\mathcal{D}(f_t(x_i), f_t(x_{m^h}))$ are template relations. [17]. Hence, with re-weighting the hardest samples, the *InfoNCE*-like loss function [28] is defined as:

$$\ell_i^{hsd} = -\log \frac{\exp(w_i^n \nu_i^n / \tau_h)}{\exp(w_i^n \nu_i^n / \tau_h) + \exp(w_i^p \nu_i^p / \tau_h)}. \quad (7)$$

Here, τ_h is a temperature hyperparameter. Through the minimization of Eq. (7), we strive to bring the hardest positive pair closer together while simultaneously pushing the hardest negative pair further apart. Moreover, the optimization described in Eq. (6) will terminate when the false-negative samples are significantly distanced from the template relation and vice versa, which will set the optimization of the incorrect pairs right. Here the template relation can be regarded as the lower bound of the worst case.

Finally, traveling N instances within a mini-batch, the total loss function of HSD is expressed as follows,

$$\mathcal{L}_{HSD} = \frac{1}{N} \sum_{i=1}^N \ell_i^{hsd}. \quad (8)$$

C. Prototypical Contrastive Learning

Although non-contrastive learning methods do not require any negative pairs, they usually lead to the collapse of downstream clustering, causing the emergence of an unstable clustering phenomenon. To avoid this collapse and guarantee stable downstream clustering, we incorporate prototypical contrastive learning (PCL) [11], [12] into our model. Similar to vanilla contrastive learning, PCL treats one prototype (i.e. cluster center) and the prototype of another view as positive pairs, while considering other prototypes as negative pairs [12].

Specifically, assume that there are K prototypes from the student embedding space, $\{u_1^s, u_2^s, \dots, u_K^s\}$ and another K prototypes from the teacher embedding space, $\{u_1^t, u_2^t, \dots, u_K^t\}$. Thus the loss function of PCL is defined as follows:

$$\mathcal{L}_{PCL} = \frac{1}{K} \sum_{k=1}^K -\log \frac{\exp((u_k^s)^T u_k^t / \tau_p)}{\exp((u_k^s)^T u_k^t / \tau_p) + \sum_{\substack{j=1 \\ j \neq k}}^K \exp((u_k^s)^T u_j^t / \tau_p)}, \quad (9)$$

where τ_p is a temperature parameter. More precisely, by leveraging the posterior probability of cluster assignment $\phi(k|x)$, the estimation of prototypes u_k^s and u_k^t within a mini-batch \mathcal{B} can be computed as follows:

$$u_k^s = \frac{\sum_{x \in \mathcal{B}} \phi(k|x) f_s(x)}{\|\sum_{x \in \mathcal{B}} \phi(k|x) f_s(x)\|_2}, \quad (10)$$

$$u_k^t = \frac{\sum_{x \in \mathcal{B}} \phi(k|x) f_t(x)}{\|\sum_{x \in \mathcal{B}} \phi(k|x) f_t(x)\|_2}. \quad (11)$$

When the number of clusters K exceeds the size of the mini-batch \mathcal{B} , it is evident that the mini-batch cannot encompass all clusters. To address this, we mitigate the issue by nullifying the losses and logits associated with empty clusters during each iteration.

In the training process, the accurate estimation of $\phi(k|x)$ plays a crucial role in optimizing the loss of prototypical contrastive learning. To achieve this goal, following ProPos [12], we utilize K -means clustering at the initial phase of each epoch while minimizing the loss function specified in Eq. (9) at the end of each epoch. Although the prototypes are not as accurate as desired during the initial epochs of training, after the completion of a learning rate warmup [11], [12], the loss of prototypical contrastive learning will be incorporated in training to ensure a more accurate initialization.

Intuitively, prototypical contrastive learning is similar to vanilla contrastive learning for instances. The main differences are that 1) prototypical contrastive learning does not require a large number of negative pairs because clusters K is definitely far smaller than the size of whole dataset, and 2) prototypical contrastive learning is more suitable for deep clustering because it encourages the prototypes to be uniformly distributed in the embedding space, which can improve the compactness of clusters.

D. Overview

We build HaDis upon a self-distillation framework similar to BYOL [3] and ProPos [12]. In the training process, the parameters of teacher network θ_t are updated with moving average from the ones of student network θ_s , which can be formulated as:

$$\theta_t = \alpha \theta_t + (1 - \alpha) \theta_s, \quad (12)$$

where $\alpha \in [0, 1)$ is the hyperparameter that controls the degree of updating for the teacher network.

Formally, as shown in Fig. 1, two different data augmentations are applied to the same image input and then two augmented views are fed into the student network and teacher network, respectively. Further, prototypical contrastive learning is leveraged to contrast the prototypes, which are generated from the student and teacher embeddings by performing K -means clustering. Simultaneously, the proposed DSA forces the student embeddings to align with that of the teacher, and HSD is proposed to perform robust hard sample learning to alleviate the sampling bias phenomenon. Ultimately, the overall loss function of HaDis to optimize is defined as follows,

$$\mathcal{L} = \mathcal{L}_{DSA} + \mathcal{L}_{HSD} + \lambda \mathcal{L}_{PCL}, \quad (13)$$

where λ is a hyperparameter. Note that in the testing process, we only take the teacher network to extract features and utilize K -means to get the final clustering results.

To help intuitively understanding the training procedure of the proposed HaDis, the pytorch-like pseudo-code is presented in Algorithm 1.

Algorithm 1: Pytorch-like pseudo-code of our HaDis.

```

# f_s: student network
# f_t: teacher network
# g: predictor
# param_s: parameters of the student network
# param_t: parameters of the teacher network
# tau: weight for labels from last epoch
# alpha, epsilon, eta, lambda: hyperparameter

# use K-means to get the pseudo-labels of all images
# train one epoch
for x in dataloader: # load a mini-batch
    # two random views
    x_s, x_t = f_s(aug(x)), f_t(aug(x))
    # compute the cluster centers
    u_s = compute_centers(x_s, pseudo_labels)
    u_t = compute_centers(x_t, pseudo_labels)
    # generate the diffused features
    d_s = x_s + randn_like(x_s)*epsilon
    # calculate the proposed losses
    loss_align = critieon_align(x_t, g(d_s))
    loss_dhds = critieon_dhds(x_t, g(d_s))
    loss_pcl = critieon_pcl(u_s, u_t) #
    # update the student network and pseudo-labels
    loss = loss_align + eta*loss_dhds + lambda*loss_pcl
    loss.backward()
    # update the teacher network via moving averaged
    param_t = param_t*alpha + param_s*(1 - alpha)

# testing
# adopt the teacher network as final encoder
# extract the features of all images
all_features = f_t(all_x)
# get predictions via K-means clustering
labels = Kmeans.fit_predict(all_features)

```

IV. EXPERIMENTS

A. Implementation Details

Following the related literature [7], [12] strictly, we adopt BigResNet-18 [12] as the backbone for all experiments. In terms of data augmentations, we take the same augmentations as SimCLR [1], which consists of ResizedCrop, ColorJitter, Grayscale and HorizontalFlip. However, GaussianBlur has been removed since we adopt only a small image size for all datasets [7], [10], [13]. In terms of mini-batch, the batch size is fixed at 256 for CIFAR-10 and CIFAR-100, and 128 for the rest of the datasets.

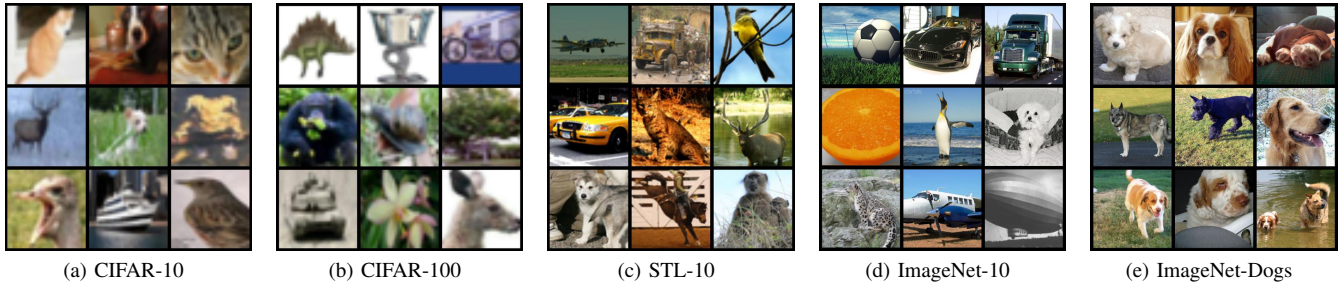


Fig. 2. Some exemplars of the five benchmark datasets.

TABLE I
THE FIVE BENCHMARK DATASETS USED IN OUR EXPERIMENTS.

Dataset	Split	#Samples	#Clusters	#Image Size
CIFAR-10	Train+Test	60,000	10	$32 \times 32 \times 3$
CIFAR-100	Train+Test	60,000	20	$32 \times 32 \times 3$
STL-10	Train+Test	13,000	10	$96 \times 96 \times 3$
ImageNet-10	Train	13,000	10	$96 \times 96 \times 3$
ImageNet-Dogs	Train	19,500	15	$96 \times 96 \times 3$

For a fair comparison, we train all clustering approaches for 1,000 epochs. Since our HaDis is built upon ProPos [12], we also utilize the stochastic gradient descent (SGD) optimizer and employ a cosine decay learning rate schedule with a 50-epoch warmup. Following BYOL [3] and ProPos [12], the base learning rate is set to 0.05, which is proportionally scaled with the batch size ($\text{LearningRate} = 0.05 \times \text{BatchSize}/256$). Notably, the learning rates for the predictor networks in HaDis are 10 times higher than that of the feature extractor.

For hyperparameters of HaDis, the temperatures τ_h and τ_p for HSD and PCL are both 0.5. The ϵ for diffused sampling is set as 0.001. As for the hyperparameters λ in Eq. (13), we finetune λ in a grid search $\{0.01, 0.05, 0.1, 0.5, 1\}$. In particular, λ is set to 0.05 for CIFAR-100 and ImageNet-10, and 0.1 for CIFAR-10, STL-10 and ImageNet-Dogs. For momentum hyperparameter $\alpha \in [0, 1)$, we set it to 0.996 in line with BYOL and ProPos. All experiments are run on an NVIDIA GeForce RTX 3090 GPU.

B. Datasets and Evaluation Metrics

In this paper, five challenging benchmark datasets for clustering are used: CIFAR-10 [35], CIFAR-100 [35], STL-10 [36], ImageNet-10 [37] and ImageNet-Dogs [37].

For clarity, we summarize the statistics of these datasets in Table I. Note that for CIFAR-100, we adopt the 20 super-classes as the ground truth for evaluation. In the case of STL-10, both labeled and unlabeled data are employed for training and evaluation.

In terms of evaluation metrics, we adopt normalized mutual information (NMI), clustering accuracy (ACC), and adjusted rand index (ARI) to evaluate the clustering performance. The higher values of these metrics indicate superior clustering results.

C. Baseline Methods

We compare the proposed HaDis with both non-deep and deep clustering methods. Specifically, we select four non-deep clustering baseline methods for comparison, including K -means [38], SC [19], AC [20] and NMF [21]. Besides, deep clustering baseline methods involves AE [22], DAE [23], DCGAN [39], DeCNN [40], VAE [41], JULE [25], DEC [24], DAC [37], DCCM [42], PICA [26], IDFD [8], CC [7], ProPos [12], HTCEN [13] and SACC [10]. We have reproduced the results of IDFD, CC and ProPos by using their official code and strictly following the suggested settings. The scores (w.r.t NMI, ACC and ARI) of the other baseline methods are obtained from the respective papers.

D. Results and Analysis

In this section, our proposed HaDis is compared against nineteen clustering baseline methods on five challenging benchmark datasets, as presented in Table II.

Concretely, our proposed HaDis achieves state-of-the-art clustering performance on the five benchmark datasets. Especially, on the CIFAR-100 dataset, the proposed HaDis attains an NMI score of 56.8, which has been a significant improvement of exactly three points compared to the second-best NMI (i.e., 53.8). In terms of ACC scores, our HaDis has achieved remarkable clustering performance on CIFAR-100, ImageNet-10 and ImageNet-Dogs, where the ACC scores are 56.3, 94.9 and 55.0, respectively. Similarly, it can be observed that our HaDis attains unprecedented top ARI scores across all datasets except STL-10.

In addition to quantitative evaluation, we also provide visual analysis of the clustering results obtained by the proposed HaDis method. As illustrated in Fig. 3, we draw the confusion matrices that depict the correspondence between ground truths and predicted labels for the five benchmark datasets. It can be observed that clear block-diagonal structures are present on CIFAR-10, STL-10 and ImageNet-10. Even for the more challenging datasets, namely, CIFAR-100 and ImageNet-Dogs datasets, albeit less distinct, block-diagonal structures can still be observed.

E. Ablation

In this section, we conduct extensive experiments of ablation analysis to validate the influence of the proposed modules

TABLE II
THE CLUSTERING PERFORMANCE (%) OF VARIOUS METHODS ON FIVE CHALLENGING IMAGE BENCHMARKS. THE BEST RESULTS ARE SHOWN IN **BOLD** AND THE SECOND BEST RESULTS ARE SHOWN IN UNDERLINE.

Dataset	CIFAR-10			CIFAR-100			STL-10			ImageNet-10			ImageNet-Dogs		
	NMI	ACC	ARI	NMI	ACC	ARI									
K-means	8.7	22.9	4.9	8.4	13.0	2.8	12.5	19.2	6.1	11.9	24.1	5.7	5.5	10.5	2.0
SC	10.3	24.7	8.5	9.0	13.6	2.2	9.8	15.9	4.8	15.1	27.4	7.6	3.8	11.1	1.3
AC	10.5	22.8	6.5	9.8	13.8	3.4	23.9	33.2	14.0	13.8	24.2	6.7	3.7	13.9	2.1
NMF	8.1	19.0	3.4	7.9	11.8	2.6	9.6	18.0	4.6	13.2	23.0	6.5	4.4	11.8	1.6
AE	23.9	31.4	16.9	10.0	16.5	4.8	25.0	30.3	16.1	21.0	31.7	15.2	10.4	18.5	7.3
DAE	25.1	29.7	16.3	11.1	15.1	4.6	22.4	30.2	15.2	20.6	30.4	13.8	10.4	19.0	7.8
DCGAN	26.5	31.5	17.6	12.0	15.1	4.5	21.0	29.8	13.9	22.5	34.6	15.7	12.1	17.4	7.8
DeCNN	24.0	28.2	17.4	9.2	13.3	3.8	22.7	29.9	16.2	18.6	31.3	14.2	9.8	17.5	7.3
VAE	24.5	29.1	16.7	10.8	15.2	4.0	20.0	28.2	14.6	19.3	33.4	16.8	10.7	17.9	7.9
JULE	19.2	27.2	13.8	10.3	13.7	3.3	18.2	27.7	16.4	17.5	30.0	13.8	5.4	13.8	2.8
DEC	25.7	30.1	16.1	13.6	18.5	5.0	27.6	35.9	18.6	28.2	38.1	20.3	12.2	19.5	7.9
DAC	39.6	52.2	30.6	18.5	23.8	8.8	36.6	47.0	25.7	39.4	52.7	30.2	21.9	27.5	11.1
DCCM	49.6	62.3	40.8	28.5	32.7	17.3	37.6	48.2	26.2	60.8	71.0	55.5	32.1	38.3	18.2
PICA	59.1	69.6	51.2	31.0	33.7	17.1	61.1	71.3	53.1	80.2	87.0	76.1	35.2	35.2	20.1
IDFD	71.1	81.5	66.3	42.6	42.5	26.4	59.6	70.3	53.2	79.7	85.4	68.5	47.0	<u>50.2</u>	34.1
CC	68.1	76.6	60.6	42.4	42.6	26.7	67.4	<u>74.7</u>	60.6	86.2	89.5	82.5	40.1	<u>34.2</u>	22.5
ProPos	<u>86.0</u>	<u>92.3</u>	<u>84.6</u>	<u>53.8</u>	<u>52.8</u>	<u>36.0</u>	68.7	73.1	61.4	84.8	90.0	81.9	45.9	47.4	33.8
HTCN	65.7	71.8	57.0	46.5	47.2	30.5	61.8	70.1	51.7	87.5	<u>90.5</u>	83.9	<u>49.4</u>	49.3	<u>35.2</u>
SACC	76.5	85.1	72.4	44.8	44.3	28.2	<u>69.1</u>	75.9	62.6	<u>87.7</u>	<u>90.5</u>	<u>84.3</u>	45.5	43.7	28.5
HaDis (Ours)	86.9	93.0	86.2	56.8	56.3	41.1	69.6	73.9	<u>62.3</u>	88.4	94.9	89.2	49.6	55.0	37.6

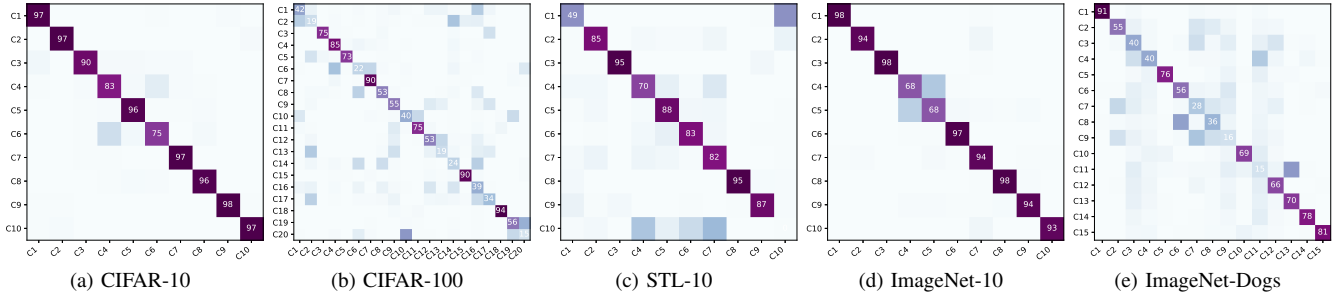


Fig. 3. The confusion matrices on the five benchmark datasets.

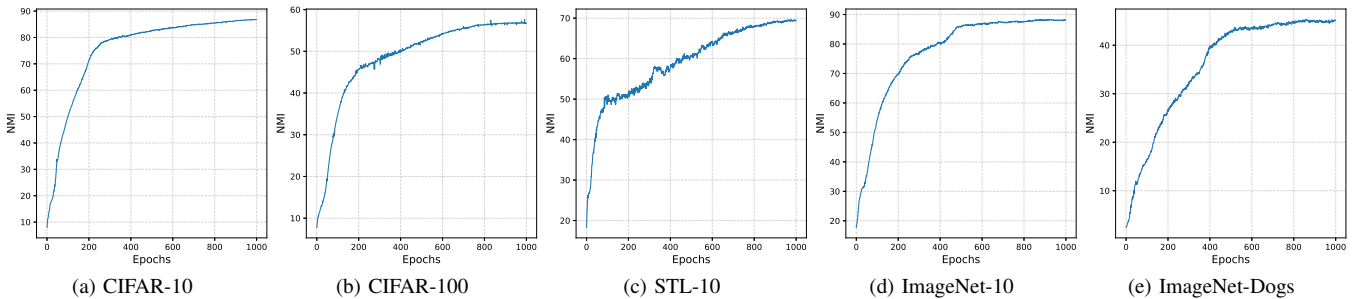


Fig. 4. The NMI (%) performance of HaDis as the number of epochs increases.

themselves and the effect of the interactions between different modules.

a) Influence of HSD and PCL.: In this ablation study, we mainly validate the influence of hardness-aware self-distillation (HSD) and prototypical contrastive learning (PCL). Table III presents the results of the ablation experiments, where HSD and PCL are systematically removed to assess

their impacts on the overall performance. Clearly, our model without PCL suffers from clustering instability and finally results in poor clustering results. Indeed, the absence of HSD in HaDis would lead to its degradation into ProPos [12], resulting in a sub-optimal performance. Only by leveraging HSD and PCL concurrently can our HaDis unleash its full potential and achieve state-of-the-art clustering results.

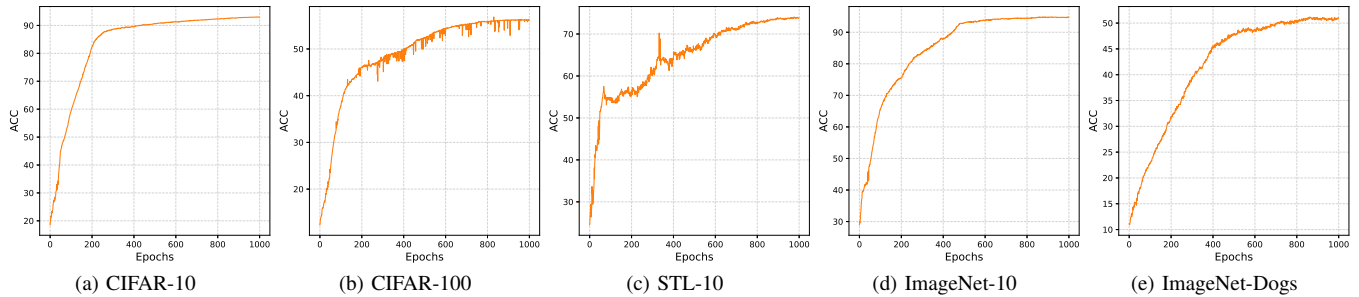


Fig. 5. The ACC (%) performance of HaDis as the number of epochs increases.

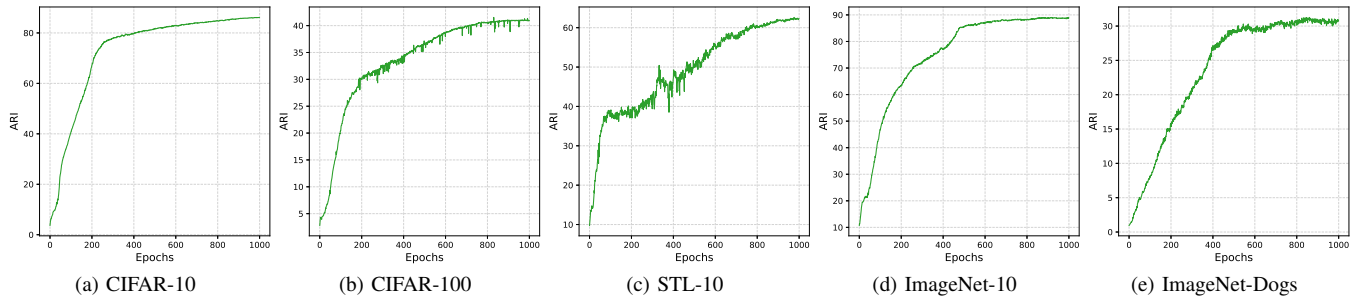


Fig. 6. The ARI (%) performance of HaDis as the number of epochs increases.

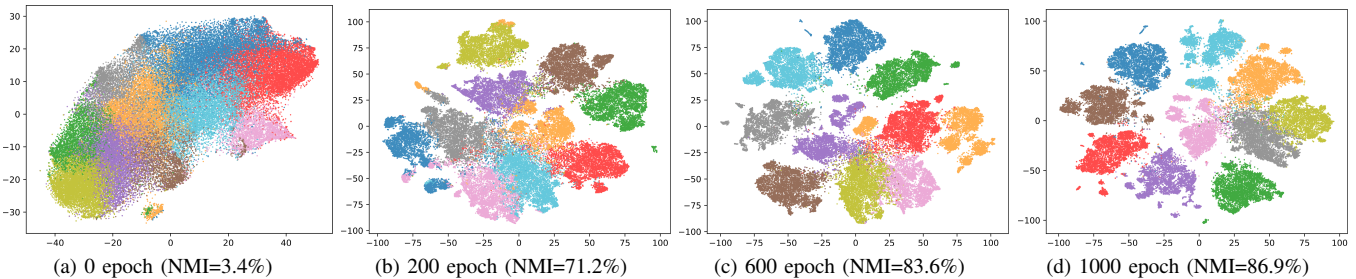


Fig. 7. The t-SNE visualization of HaDis on CIFAR-10.

TABLE III
THE INFLUENCE OF HSD AND PCL. THE BEST RESULTS ARE SHOWN IN BOLD.

Dataset	PCL	HSD	NMI	ACC	ARI
CIFAR-10	✓	✗	85.8	92.0	84.3
	✗	✓	78.5	86.0	73.9
	✓	✓	86.9	93.0	86.2
ImageNet-10	✓	✗	85.0	90.3	82.9
	✗	✓	83.3	92.0	83.4
	✓	✓	88.4	94.9	89.2

TABLE IV
THE INFLUENCE OF DIFFUSED SAMPLING ON CIFAR-10. THE BEST RESULTS ARE SHOWN IN BOLD.

Method	NMI	ACC	ARI
HaDis ($\epsilon = 0$)	83.9	91.1	82.4
HaDis ($\epsilon = 0.001$)	86.9	93.0	86.2
HaDis ($\epsilon = 0.005$)	85.3	91.9	83.8
HaDis ($\epsilon = 0.01$)	83.4	90.3	80.9

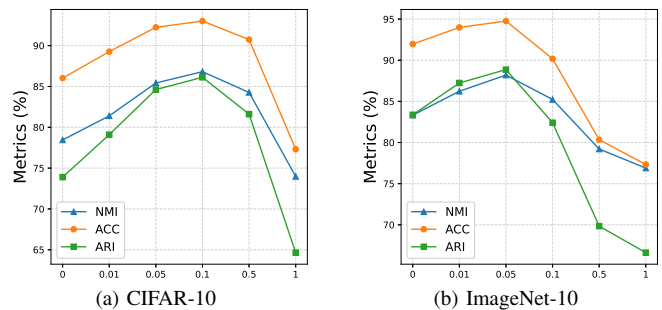


Fig. 8. The influence of hyperparameter λ for PCL on CIFAR-10 and ImageNet-10.

b) Influence of Diffused Sampling.: The hyperparameter ϵ controls the range of diffused sampling. In Table IV, it can be observed that introducing the diffused sampling into our model, setting ϵ as 0.001 significantly leads to performance improvements on CIFAR-10. However, when ϵ is set excessively large, the clustering performance experiences a salient drop. This outcome is expected because, with a large ϵ , those

false positive samples may be considered as true positives.

c) *Influence of Hyperparameter λ* : The hyperparameter λ determines the importance of PCL, which controls the dispersion level between intra-cluster. The results in Fig. 8 indicate that both excessively large or small values of λ would result in a decrease in clustering performance, particularly in terms of ACC and ARI. Nevertheless, it is suggested that λ can be set to $[0.05, 0.1]$, as it has been demonstrated to yield superior performance on CIFAR-10 and ImageNet-10, respectively.

F. Convergence Analysis

In this section, we assess the convergence behavior of the proposed HaDis method. Specifically, we record the NMI, ACC, and ARI scores for every single epoch and present them in Figs. 4, 5 and 6. Obviously, the clustering performance (w.r.t NMI, ACC and ARI) exhibit a consistent upward trend as the number of epochs increases. Notably, our HaDis achieves high-quality clustering results on most datasets when the number of epochs surpasses 600. From the perspective of training stability, our HaDis exhibits remarkable stability on CIFAR-10, ImageNet-10, and ImageNet-Dogs datasets, where it is evident from the smooth and consistent curves of various metrics. Especially, we think that the substantial fluctuations on CIFAR-100 and STL-10 can likely be attributed to the inherent characteristics and data distribution of these datasets. Indeed, the CIFAR-100 dataset contains small and blurry images, making it challenging to discern fine-grained details. As for STL-10, the presence of a large number of unlabeled images and the unconventional training process contribute to the significant fluctuations in clustering performance.

Furthermore, we employ t-SNE [43] to visualize the convergence of the HaDis method on the learned representations of the CIFAR-10 dataset. The six different timestamps throughout the training process are shown in Fig. 7, where different colors denote different labels predicted by K -means clustering. The results reveal that the features are mixed initially, but as the training progresses, the cluster assignments gradually become more coherent and aligned with the underlying data structure.

V. CONCLUSION

In this paper, we propose a novel end-to-end deep clustering framework, termed HaDis. We propose diffused sampling alignment and hardness-aware self-distillation to enhance clustering performance and mitigate the sample bias phenomenon. By incorporating prototypical contrastive learning, our proposed HaDis owns several remarkable advantages, including an exclusion of massive negative pairs, robust clustering stability, pretraining-free knowledge learning, and unbiased representation learning. Extensive experiments on five benchmark datasets demonstrate the superiority of our proposed approach.

REFERENCES

- [1] T. Chen, S. Kornblith, M. Norouzi, and G. Hinton, "A simple framework for contrastive learning of visual representations," in *Proc. of International Conference on Machine Learning (ICML)*, 2020.
- [2] K. He, H. Fan, Y. Wu, S. Xie, and R. Girshick, "Momentum contrast for unsupervised visual representation learning," in *Proc. of IEEE Conference on Computer Vision and Pattern Recognition (CVPR)*, 2020.
- [3] J.-B. Grill, F. Strub, F. Altché, C. Tallec, P. Richemond, E. Buchatskaya, C. Doersch, B. Avila Pires, Z. Guo, M. Gheshlaghi Azar *et al.*, "Bootstrap your own latent—a new approach to self-supervised learning," in *Advanced in Neural Information Processing Systems (NeurIPS)*, 2020.
- [4] X. Chen and K. He, "Exploring simple siamese representation learning," in *Proceedings of the IEEE/CVF conference on computer vision and pattern recognition*, 2021, pp. 15 750–15 758.
- [5] M. Caron, I. Misra, J. Mairal, P. Goyal, P. Bojanowski, and A. Joulin, "Unsupervised learning of visual features by contrasting cluster assignments," in *Advanced in Neural Information Processing Systems (NeurIPS)*, 2020.
- [6] W. Van Gansbeke, S. Vandenhende, S. Georgoulis, M. Proesmans, and L. Van Gool, "Scan: Learning to classify images without labels," in *Computer Vision—ECCV 2020: 16th European Conference, Glasgow, UK, August 23–28, 2020, Proceedings, Part X*. Springer, 2020, pp. 268–285.
- [7] Y. Li, P. Hu, Z. Liu, D. Peng, J. T. Zhou, and X. Peng, "Contrastive clustering," in *Proc. of AAAI Conference on Artificial Intelligence (AAAI)*, 2021.
- [8] Y. Tao, K. Takagi, and K. Nakata, "Clustering-friendly representation learning via instance discrimination and feature decorrelation," *arXiv preprint arXiv:2106.00131*, 2021.
- [9] C. Niu, H. Shan, and G. Wang, "Spice: Semantic pseudo-labeling for image clustering," *IEEE Transactions on Image Processing*, vol. 31, pp. 7264–7278, 2022.
- [10] X. Deng, D. Huang, D.-H. Chen, C.-D. Wang, and J.-H. Lai, "Strongly augmented contrastive clustering," *Pattern Recognition*, vol. 139, p. 109470, 2023.
- [11] J. Li, P. Zhou, C. Xiong, and S. C. Hoi, "Prototypical contrastive learning of unsupervised representations," *arXiv preprint arXiv:2005.04966*, 2020.
- [12] Z. Huang, J. Chen, J. Zhang, and H. Shan, "Learning representation for clustering via prototype scattering and positive sampling," *IEEE Transactions on Pattern Analysis and Machine Intelligence*, pp. 1–16, 2022. [Online]. Available: <https://doi.org/10.1109/2Ftpami.2022.3216454>
- [13] X. Deng, D. Huang, and C.-D. Wang, "Heterogeneous tri-stream clustering network," *Neural Processing Letters*, pp. 1–14, 2023.
- [14] C.-Y. Chuang, J. Robinson, Y.-C. Lin, A. Torralba, and S. Jegelka, "Debiased contrastive learning," *Advances in neural information processing systems*, vol. 33, pp. 8765–8775, 2020.
- [15] H. Zhao, X. Yang, Z. Wang, E. Yang, and C. Deng, "Graph debiased contrastive learning with joint representation clustering," in *IJCAI*, 2021, pp. 3434–3440.
- [16] F. Wang and H. Liu, "Understanding the behaviour of contrastive loss," in *Proceedings of the IEEE/CVF conference on computer vision and pattern recognition*, 2021, pp. 2495–2504.
- [17] H. Liu and M. Ye, "Improving self-supervised lightweight model learning via hard-aware metric distillation," in *European Conference on Computer Vision*. Springer, 2022, pp. 295–311.
- [18] S. Abbasi Koohpayegani, A. Tejankar, and H. Pirsiavash, "Compress: Self-supervised learning by compressing representations," *Advances in Neural Information Processing Systems*, vol. 33, pp. 12 980–12 992, 2020.
- [19] L. Zelnik-Manor and P. Perona, "Self-tuning spectral clustering," in *Advanced in Neural Information Processing Systems (NeurIPS)*, 2005.
- [20] K. C. Gowda and G. Krishna, "Agglomerative clustering using the concept of mutual nearest neighbourhood," *Pattern Recognition*, vol. 10, no. 2, pp. 105–12, 1978.
- [21] D. Cai, X. He, X. Wang, H. Bao, and J. Han, "Locality preserving non-negative matrix factorization," in *Proc. of International Joint Conference on Artificial Intelligence (IJCAI)*, 2009.
- [22] Y. Bengio, P. Lamblin, D. Popovici, and H. Larochelle, "Greedy layer-wise training of deep networks," *Advances in Neural Information Processing Systems*, vol. 19, 2006.
- [23] P. Vincent, H. Larochelle, I. Lajoie, Y. Bengio, P.-A. Manzagol, and L. Bottou, "Stacked denoising autoencoders: Learning useful representations in a deep network with a local denoising criterion." *Journal of Machine Learning Research*, vol. 11, no. 12, 2010.
- [24] J. Xie, R. Girshick, and A. Farhadi, "Unsupervised deep embedding for clustering analysis," in *Proc. of International Conference on Machine Learning (ICML)*, 2016.

- [25] J. Yang, D. Parikh, and D. Batra, "Joint unsupervised learning of deep representations and image clusters," in *IEEE Conference on Computer Vision and Pattern Recognition*, 2016, pp. 5147–5156.
- [26] J. Huang, S. Gong, and X. Zhu, "Deep semantic clustering by partition confidence maximisation," in *IEEE/CVF Conference on Computer Vision and Pattern Recognition*, 2020, pp. 8849–8858.
- [27] Z. Wu, Y. Xiong, S. X. Yu, and D. Lin, "Unsupervised feature learning via non-parametric instance discrimination," in *Proceedings of the IEEE conference on computer vision and pattern recognition*, 2018, pp. 3733–3742.
- [28] A. v. d. Oord, Y. Li, and O. Vinyals, "Representation learning with contrastive predictive coding," *arXiv preprint arXiv:1807.03748*, 2018.
- [29] J. Robinson, C.-Y. Chuang, S. Sra, and S. Jegelka, "Contrastive learning with hard negative samples," *arXiv preprint arXiv:2010.04592*, 2020.
- [30] Y. Kalantidis, M. B. Sariyildiz, N. Pion, P. Weinzaepfel, and D. Larlus, "Hard negative mixing for contrastive learning," *Advances in Neural Information Processing Systems*, vol. 33, pp. 21 798–21 809, 2020.
- [31] J. Xia, L. Wu, G. Wang, J. Chen, and S. Z. Li, "Progcl: Rethinking hard negative mining in graph contrastive learning," *arXiv preprint arXiv:2110.02027*, 2021.
- [32] Y. Liu, X. Yang, S. Zhou, X. Liu, Z. Wang, K. Liang, W. Tu, L. Li, J. Duan, and C. Chen, "Hard sample aware network for contrastive deep graph clustering," in *Proceedings of the AAAI conference on artificial intelligence*, vol. 37, no. 7, 2023, pp. 8914–8922.
- [33] Y. Tian, X. Chen, and S. Ganguli, "Understanding self-supervised learning dynamics without contrastive pairs," in *International Conference on Machine Learning*. PMLR, 2021, pp. 10 268–10 278.
- [34] M. Ye, H. Li, B. Du, J. Shen, L. Shao, and S. C. Hoi, "Collaborative refining for person re-identification with label noise," *IEEE Transactions on Image Processing*, vol. 31, pp. 379–391, 2021.
- [35] A. Krizhevsky, G. Hinton *et al.*, "Learning multiple layers of features from tiny images," 2009.
- [36] A. Coates, A. Ng, and H. Lee, "An analysis of single-layer networks in unsupervised feature learning," in *Proceedings of the fourteenth international conference on artificial intelligence and statistics*. JMLR Workshop and Conference Proceedings, 2011, pp. 215–223.
- [37] J. Chang, L. Wang, G. Meng, S. Xiang, and C. Pan, "Deep adaptive image clustering," in *Proceedings of the IEEE international conference on computer vision*, 2017, pp. 5879–5887.
- [38] J. MacQueen *et al.*, "Some methods for classification and analysis of multivariate observations," in *Proc. of Mathematical Statistics and Probability*, 1967.
- [39] A. Radford, L. Metz, and S. Chintala, "Unsupervised representation learning with deep convolutional generative adversarial networks," *arXiv preprint arXiv:1511.06434*, 2015.
- [40] M. D. Zeiler, D. Krishnan, G. W. Taylor, and R. Fergus, "Deconvolutional networks," in *IEEE Conference on Computer Vision and Pattern Recognition*, 2010, pp. 2528–2535.
- [41] D. P. Kingma and M. Welling, "Auto-encoding variational bayes," *arXiv preprint arXiv:1312.6114*, 2013.
- [42] J. Wu, K. Long, F. Wang, C. Qian, C. Li, Z. Lin, and H. Zha, "Deep comprehensive correlation mining for image clustering," in *IEEE/CVF International Conference on Computer Vision*, 2019, pp. 8150–8159.
- [43] L. Van der Maaten and G. Hinton, "Visualizing data using t-sne," *Journal of machine learning research*, vol. 9, no. 11, 2008.